sustainability

MDPI

Article

Production and Compression Strength of Mortars Containing Unprocessed Waste Powdered Steel Slag

Stefano Maschio, Eleonora Aneggi, Lorenzo Fedrizzi, Francesco Andreatta, Maria Lekka, Alex Lanzutti and Erika Furlani *

Polytechnic Department of Engineering and Architecture, University of Udine, Via del Cotonificio 108, 33100 Udine, Italy; stefano.maschio@uniud.it (S.M.); eleonora.aneggi@uniud.it (E.A.); lorenzo.fedrizzi@uniud.it (L.F.); francesco.andreatta@uniud.it (F.A.); maria.lekka@uniud.it (M.L.); alex.lanzutti@uniud.it (A.L.)

* Correspondence: erika.furlani@uniud.it; Tel.: +39-432-558-863

Received: 23 November 2017; Accepted: 17 December 2017; Published: 19 December 2017

Abstract: This paper deals with the production of mortars prepared using a commercial CEMIIB-S 42.5N cement, a natural aggregate, steelmaking slag, a superplasticizer and water. The as-received unprocessed steel slag was milled by a hammer mill and then sieved to obtain batches with different maximum particle size. Each batch was used, together with the other components, in the production of mortars which were tested, by compression and water absorption, after different aging times in order to evaluate their long term stability. Several slag-free samples were also prepared as reference materials. All mortars were prepared with fixed aggregate/cement ratio (6/1), superplasticizer/cement ratio (s/c) and water/cement ratio (w/c). It has been demonstrated that an adequate protocol for the preparation and the use of slag containing particles with 2500 μm maximum size lead to the production of materials with mechanical properties suitable for civil engineering applications after aging for 28, 90 and 180 days. However, samples containing slag particles with size equal or greater than 1000 μm display a decay of mechanical properties after longer aging in water or after accelerated aging.

Keywords: mortar; unprocessed steel slag; long time aging; compressive strength

1. Introduction

Steelmaking slag (SS) derives from the high temperature production process of steel and is unstable due to its high content of lime. This is mainly related to the presence of $2CaO\text{-}SiO_2$, which can transform, during cooling or successive aging, into a phase with larger specific volume [1] crumbling the slag. This results in a mixture of submicronic and micronic-granulated particles. Moreover, the residual free lime can spontaneously hydrate in the atmospheric environment after cooling. Both of the above volumetric instabilities represent a drawback when slag is used as a raw material for recycling. In addition, the volumetric instabilities can be combined with a retarded hydration when slags containing free MgO or MgO-based compounds are used in the production of mortars or concretes [2–5]. It is generally accepted that a better stability could be obtained when the slag is pre-treated by different methods such as long time weathering of the granulated slag outside the slag pits, treatment of the liquid slag by injecting oxygen and silica, autoclaving of the slag in baskets [6,7] and others [8–10].

The extremely large quantity of SS produced all over the world by steel industries represents a strong driving force for recycling of this byproduct of steel production. However, recycling of SS could be convenient provided that the produced materials possess good durability and maintain properties in line with the requirements of standards after long time aging.

In this view, several authors proposed the use of blended cements containing SS for concrete manufacturing [11–13]. For this specific application, SS needs to be converted by milling into a powdered product. Blending could be reasonably performed by cement industries in order to scale up the process at industrial level.

Other authors found that cement-based materials with good properties could be obtained when SS are employed as partial replacement of sand fines with optimized replacement ratios [3,4,14–18]. In addition, Shi [19,20] observed that ladle slag fines showed significant cementitious behaviour in the presence of an alkaline activator and that the cementitious properties became more evident decreasing the size of the slag particles. On the other hand, Qasrawi et al. [18] showed that the use of steel slag as fine aggregate had a negative impact on workability. Nevertheless, they evidenced a positive effect on compressive and tensile strength for aggregate replacement fractions between 15% and 30%.

It is clear that, when used as aggregate, SS processing and use could be carried out by concrete or mortars manufacturers avoiding involvement of cement industries in the SS recycling.

Independently of their chemical composition, SS normally displays a wide particle size distribution. This is affected by the slag origin, the steel production process and the time elapsed from slag generation. SS morphology is an additional parameter that must be taken into account during the preparation of mortars or concretes.

Nowadays, the use of SS containing small and coarse particles for mortar or concrete production is still under debate. However it is generally accepted that the use of powdered SS containing particles of a size equal or larger than 2.5 mm could compromise the long term durability of the material, as was demonstrated by Manso et al. [17] and Furlani and Maschio [21]. On the other hand, there is a lack of literature regarding long term durability of concretes or mortars containing unprocessed SS. The goal of the present research is to evaluate the critical SS maximum size below which mortars or concrete are not affected by long term volumetric instabilities.

This paper deals with the long term compressive strength of mortars containing cement, a natural aggregate, superplasticizer, water and SS. Samples were produced replacing 1/3 of natural aggregate with an equivalent amount of slag. Materials investigated were produced varying the maximum SS particle size. A slag-free composition was prepared to produce reference samples. All mortars were prepared with a fixed aggregate/cement ratio (6/1), as has been often proposed in literature [18,22–24], a fixed superplasticizer/cement ratio (s/c) and a fixed water/cement ratio (w/c). Materials were aged in water for different times up to the limit of 1100 days. In addition, a test after an autoclave treatment was also performed in order to compare long term aging in water with accelerated aging under pressure.

2. Materials and Methods

2.1. Materials

Starting materials for mortar preparation were: a commercial CEMIIB-S 42.5N cement; the polycarboxylic ether based superplasticizer Glenium 51 (BASF: Ludwigshafen am Rhein, Germany); a natural aggregate with a nominal maximum particle size of 2.5 mm, a steel slag (obtained from the production of a chromium-manganese austenitic steel by a rotary kiln) and water.

2.2. Characterization of the Starting Materials

The slag was used as it was produced without any previous wetting, weathering or other aging treatment. The as-received material was simply dry milled using a hammer mill in order to reduce under 5 mm the maximum particle size. The granulated product was used as source to produce four separated batches of powders having different maximum particle size: the first was obtained by a cut off with a 250 μm sieve, the second with 500 μm, the third with 1000 and the fourth with 2500 μm. In the present paper the mortars containing the four batches of SS are identified by the symbols S250, S500, S1000 and S2500. Mortars mix proportions are reported in Table 1.

Table 1. Mortars mix proportions.

	R	S2500	S1000	S500	S250
Cement (g)	330	330	330	330	330
Natural aggregate (g)	2000	1500	1500	1500	1500
s/c	0.01	0.01	0.01	0.01	0.01
w/c	0.35	0.35	0.35	0.35	0.35
Slag (Ø < 2500 μm) (g)	-	500	-	-	-
Slag(Ø < 1000 μm) (g)	-	-	500	-	-
Slag (Ø < 500 μm) (g)	-	-	-	500	-
Slag (Ø < 250 μm) (g)	-	-	-	-	500

The chemical analysis of natural aggregate, slag and cement, determined by a Spectro Mass 2000 induced coupled plasma (ICP) mass spectrometer is reported, in terms of oxides, in Table 2. The amount of free lime in the slag was also determined following the ethylene glycol method. The density was determined following the ASTM C127 and C128 standards.

Table 2. Composition, Loss on ignition (LOI) and density of CEMII/B-S, natural aggregate and SS. "Others" indicates the cumulative quantity of all oxides determined in quantities lower than 0.1 wt %.

Component	CEMIIB-S (wt %)	Natural Aggregate (wt %)	SS (wt %)
CaO	55.9	55.3	38.9
SiO_2	26.2	10.1	15.0
Al_2O_3	6.6	1.1	6.7
MgO	3.0	27.7	11.6
Na_2O	0.5	0.9	-
K_2O	1.0	0.5	-
Fe_2O_3	3.1	2.2	10.2
MnO	0.4	-	11.3
Cr_2O_3	-	-	1.8
V_2O_5	-	-	0.6
P_2O_5	0.3	-	0.9
SO_4^-	0.7	-	-
Others	2.3	2.2	3.0
Free Lime *	-	-	1.9
LOI (%)	0.25	21.7	0.15
Density (g/cm^3)	2.51	2.45	3.30

* The amount of free CaO was measured following the ethylene glycol method.

Crystalline phases of slag and cement were investigated by X-ray diffraction (XRD). XRD patterns were recorded by means of a Philips X'Pert diffractometer operating at 40 kV and 40 mA using Ni-filtered Cu-Kα radiation. Spectra were collected using a step size of 0.02° and a counting time of 40 s per angular abscissa in the range of 10–100°. The Philips X'Pert HighScore software (Philips: Amsterdam, The Netherlands) was used for phase identification and their semi-quantitative evaluation was performed following the Reference Intensity Ratio (RIR) method [25].

2.3. Mortars Preparation

A 5 L Hobart planetary according to ASTM C305 standard was employed for the mixture preparation. The amount of water was determined by the ASTM C230-BS4551 slump test using a hand operated flow table for the reference blend (R) containing cement, natural aggregate, water and superplasticizer. Due to the low cement/aggregate ratio (1/6) and to the low quantity of fines in the aggregate, the paste of the reference blend had low fluency and was classified as plastic. The w/c ratio of this blend was 0.35. The same ratio was employed for all compositions considered in this work.

All mortar pastes were prepared according to the following protocol. Initially, the aggregate and the slag were mixed for 15 min with water and superplasticizer. This rather long stirring time should

enable hydration of the hydraulic compounds of the slag. Successively, the cement was added to the mixture and the product was mixed for 5 min. Pastes were then poured under vibration into moulds with size of 100 × 100 × 100 mm (for compression tests) or 40 × 40 × 40 mm (for water absorption tests). The moulds were sealed with a plastic film to ensure mass curing and aged 48 h for a first hydration. Samples were then de-moulded, cured in air for 24 h and then in water at room temperature for 7, 28, 90, 180, 360, 720 and 1100 days. Aging was performed separately for each composition in order to avoid contamination between the different samples. The water employed for aging was maintained at a constant temperature of 25 °C (±3 °C) and replaced with fresh water every 7 days. After curing, the samples were dried with a cloth and aged in the atmosphere for 24 h in order to proceed with their characterization. In addition a complete set of samples was submitted to autoclave processing in order to obtain an accelerated aging.

2.4. Characterization of Hydrated Materials

Compression tests were performed according to ASTM C39 standard using a Test Mark CM8000 apparatus. The data were averaged over 3 measurements for each sample.

A modified ASTM C 642 standard was used to test water absorption of the hydrated samples. After curing, the samples were placed in an oven at 80 ± 5 °C for 24 h and weighted (W1). Successively, the samples were aged in an autoclave at 120 °C and 2 kPa for 2 h using 2 L of water, cooled down to room temperature (in water) and dried with a cloth and weighted again (W2). Water absorption was evaluated using the following equation:

$$W\ (\%) = 100\ (W2 - W1)/W1 \quad (1)$$

Three cubic specimens for each composition cured in water for 28 days were further subjected to an autoclave test in moist environment under the same conditions indicated above. After autoclave processing, the samples were dried for 24 h at 80 °C and subjected to compressive strength tests. This test is inspired by the ASTM C-151, which is generally used to detect the presence of expansive compounds, such as free lime or free magnesia in Portland cement, that cause the instability of the SS. The test, as performed in the present investigation, is severe and enables the evaluation of the stability/durability of the material.

In addition, three cubic specimens for each composition (cured in water for 28 days) were further subjected to 100 freezing and thawing cycles between −20° and +40 °C. Also these samples underwent compressive tests.

The expansion of 100 × 100 × 100 mm cubic samples was measured by means of a caliper before the compression tests and after 28 days curing.

3. Results

In line with the work of other researchers [26], due to the non negligible CaO + MgO content of the slag, it was decided to use a CEMIIB-S cement in order to retard the hydration process with respect to an Ordinary Portland Cement (OPC). It was expected that the use of this cement could amplify the pozzolanic effect during hydration and during the first stage of mortar aging and therefore, lead to an optimized hydration of most hydraulic compounds contained in the slag powders. Such compounds, if present in the fine fraction of the slag, can contribute to expansion during the first hydration step when materials are not yet hardened [3,4]. However, the hydration process can be difficult to control when the hydraulic components of the slag are present in clusters. This can lead to uncontrollable hydration that could occur in the hardened materials. The reduction of the maximum particles size below 2500 μm enables to optimize the contact with water during the stirring steps of mortar preparation, minimizing the risk of uncontrollable hydration.

Table 2 shows that the slag contains large amounts of CaO, SiO_2, Fe_2O_3, MgO, MnO and Al_2O_3. Other oxides have been detected in lower quantities, even if the amount of Cr_2O_3 cannot be considered negligible. The absence of relevant amounts of toxic elements can also be highlighted. In addition,

Table 2 shows that free lime is 1.7% and the ratio (CaO + MgO)/SiO_2 is above 1.4 indicating that hydraulic activity could be expected for the slag [26–29]. It can be also observed that the density is 3.30 g/cm^3, in line with values reported by other researchers [13,18,30]. The CEMIIB-S 42.5N conforms to EN-197-1 European Standards whereas natural aggregate is a mixture of calcite and dolomite.

Figure 1a shows the XRD pattern of the CEMIIB-S 42.5N cement used for mortars preparation whereas Figure 1b displays that of the as received slag. As can be seen in Figure 1a, tricalcium silicate (PDF 00-042-0551, 3CaO SiO_2), tetracalcium aluminum ferrite (PDF 01-074-0803, 4CaO Fe_2O_3 Al_2O_3), calcium aluminate (PDF 00-033-0251, $Ca_3Al_2O_6$) and quartz (PDF 01-087-2096, SiO_2) are present in the cement. The RIR investigation method also revealed the quantity of each phase: tricalcium silicate 68%, tetracalcium aluminum ferrite 8%, calcium aluminate 9% and quartz 15%. These values are in line with the UNI EN 197-1 European Standards.

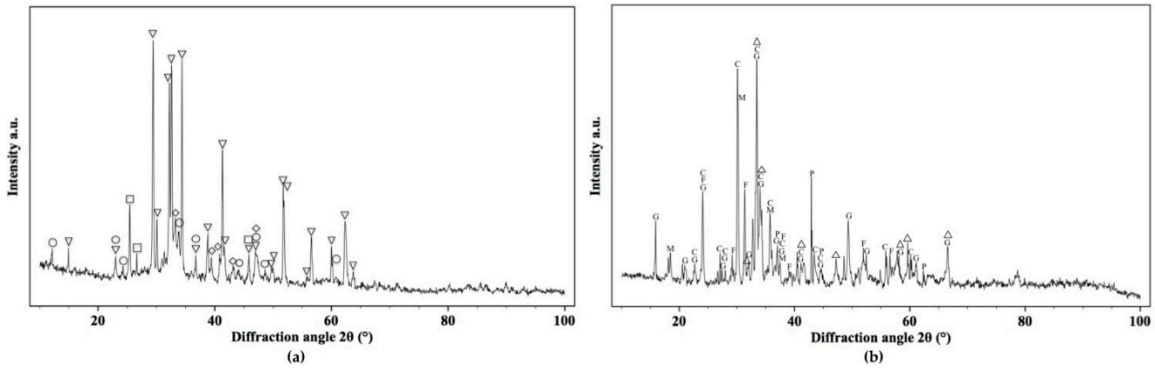

Figure 1. X-ray diffraction patterns of (**a**) CEMIIB-S and (**b**) slag. The cement contains Tricalcium silicate (∇), Calcium aluminum ferrite (○), Tricalcium aluminate (◊) and Quartz (□). Slag contains: Glaucochroite (G), Aluminum calcium oxide (Δ), Fayalite (F), Calcium Iron oxide (C), Magnetite (M) and Periclase (P).

The XRD analysis of the as-received starting slag shows the presence of several phases, some of them in very small amounts rendering very difficult their identification. Only the phases that were identified by a minimum of four representative peaks are considered in the present paper. In particular, the XRD spectrum in Figure 1b reveals the presence of aluminum calcium oxide (PDF 01-070-0134, $Ca_3Al_2O_6$), fayalite (PDF 01-080-0945, Fe_2SiO_4), glaucochroite (PDF 01-083-1745, $(Ca,Mn)_2SiO_4$), calcium iron oxide (PDF 01-072-0890, $CaOFe_2O_3$), magnetite (PDF 01-074-1910, Fe_3O_4) and periclase (PDF 00-004-0829, MgO). These phases were identified in each powder batch independently of their particles size distribution. However, it should be considered that the fraction of each phase changes for each batch as it is shown in Table 3. It can be observed that the fayalite and magnetite contents are almost constant in the four batches, while the amount of other compounds can significantly change. In particular, the amount of glaucochroite and calcium iron oxide decrease with increasing the maximum particle size of the powders whereas that of aluminum calcium oxide and periclase tend to increase in agreement with literature data [31]. The variability of the content of these compounds can affect workability as well as durability of the mortars with a negative effect on their performance.

Table 3 shows that the four batches of slag powders do not contain free CaO, and seems to be in conflict with the results obtained by the chemical analysis (see Table 2). However, this discrepancy can be attributed to the semi quantitative nature of XRD analysis, which can be less precise when crystal phases are present in traces. The presence of CaO and MgO containing phases in the slag is due to the high temperature decomposition of the dolomite, which is used as slag forming medium during steel production. It is also generally accepted that these phases can react with other components of the slag to form mixed oxides during steel production. This is clearly documented by the XRD analysis. However, the absence of free CaO in combination with the increasing amount of periclase for large maximum particle sizes indicates that CaO preferentially reacts with other components to form mixed

oxides. In contrast, MgO is less prone to react with other oxides forming large clusters of single oxide, which is associated to an increase of the size of the oxide particles.

Table 3. Phases fraction (%), identified by the RIR investigation method, mean pore size and specific surface areas of the four batches of slag powders as a function of their maximum particles dimension.

	S250	S500	S1000	S2500
Fayalite	9	8	9	8
Glaucochroite	19	17	15	14
Aluminum calcium oxide	47	50	56	58
Calcium iron oxide	21	18	10	8
Periclase	3	5	7	10
Magnetite	1	2	3	2
Pore size (nm)	12.2	11.7	12.0	11.9
Specific surface area (m^2/g)	0.9	0.7	0.8	0.7

In addition, Table 3 reports the pore size and the specific surface area of the different batches of slag. The values of pore size and specific surface areas are almost constant and appear independent on the maximum particle size: it follows that in the present discussion, their influence on materials performances was assumed to be not relevant.

As reported in the experimental section, the reference composition presented low fluidity and was classified as plastic. This behaviour forced us to vibrate the paste under casting. However, it has also been observed that mortars' workability improves decreasing the size of slag particles, as confirmed by the slump flow tests (data displayed in Table 4). This ranges from the grade of plastic (reference composition) to that of fluid (composition containing the slag with maximum size of 250 μm). This behaviour may be explained by Figure 2, which displays the cumulative particle size distribution, taking into account the excess of fines in each aggregate, according to the Bolomey equation, for the reference composition and for the S2500 and S250 ones. The trends of S500 and S1000 compositions is not shown. However, it was observed that the behaviour of these compositions was between that of S250 and S2500 compositions. It may be observed that, by replacing the natural aggregate with the slag, the trend changes toward the ideal distribution regarding workability.

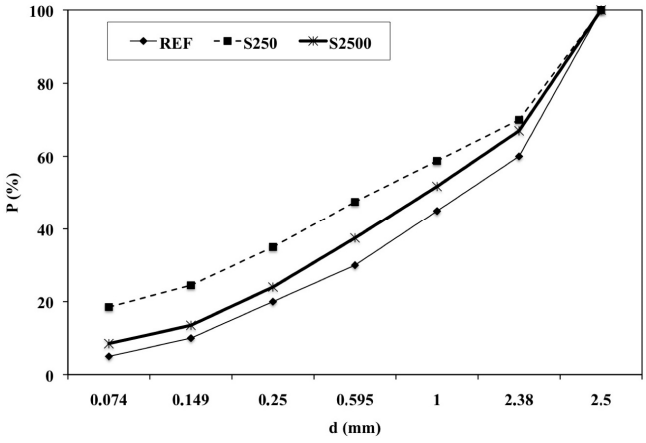

Figure 2. Cumulative particle size distribution of the reference composition and those of S250 and S2500, that has been built up taking into account the excess of fines in agreement with the Bolomey equation.

Table 4. Spread test values.

	S250	S500	S1000	S2500	R
Spread (mm)	185	165	150	130	115

In addition, it has been observed that the workability of the paste is affected by the residual porosity of the mortars. In particular, a high workability is associated with a low residual porosity. This aspect will be further discussed in the remaining part of the paper.

Figure 3 shows the compressive strength (Figure 3a) and the water absorption (Figure 3b) of samples tested after 7, 28, 90, 180, 270, 360 and 1100 days (error bars are also reported for the compressive strength).

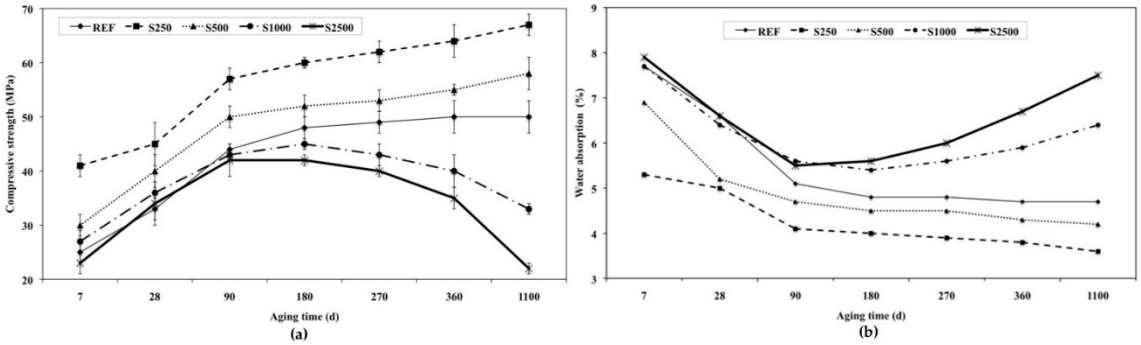

Figure 3. Compressive strength (**a**) and water absorption (**b**) as a function of aging time.

Figure 3a shows that the reference composition displays a strength of 25 MPa after 7 days, 33 MPa after 28 days increasing to 44 MPa after 90 days, 48 MPa after 180 days and remains almost constant for longer aging times (50 MPa after 1100 days). These values are relatively low for mortars prepared using a CEMIIB-S 42.5N cement. However, these can be associated with the cement/aggregate ratio (1/6) used in the present research work.

The average strength of the material with composition S250 is 41 MPa after 7 days, 45 MPa after 28 days, 57 MPa after 90 days, 60 MPa after 180 days, 62 MPa after 270 days, 64 MPa after 360 days and 67 MPa after 1100 days. This composition highlights a pozzolanic effect, which is revealed by a strong increase of strength for long aging times.

The average compressive strength of composition S500 is 30 MPa after 7 days, 40 MPa after 28 days, 50 MPa after 90 days, 52 MPa after 180 days, 53 MPa after 270 days, 55 MPa after 360 days and 58 MPa after 1100 days. It can be assumed that the pozzolanic phenomenon also affects the mechanical properties of this composition.

The composition S1000 exhibits an average strength of 27 MPa after 7 days, 36 MPa after 28 days, 43 MPa after 90 days and 45 MPa after 180 days. For longer aging times, its average strength progressively decreases, reaching 33 MPa after 1100 days. This indicates that the material suffers from a certain instability after 180 days of aging, due to retarded hydration reactions of some components introduced with the slag. A similar trend can be observed for the composition S2500, which displays an increase of strength for aging up to 180 days (42 MPa) followed by a marked decrease for longer aging times (22 MPa after 1100 days of aging).

The trend of the compressive strength shown in Figure 3 highlights that materials containing slag with maximum size equal or smaller than 500 μm exhibit different behaviour than those with larger slag particles (equal or larger than 1000 μm). In the case of small sized slag particles, complete hydration can be achieved during the first stage of mortars aging when materials are still not completely hardened. In contrast, the presence of large slag particles delay the hydration reactions which in turns lead to expansion and then cracking of the hydrated materials. This is associated with a marked reduction of the strength of the material (Figure 3), in line with the results reported in a previous work [21]. Moreover, slag particles with maximum size equal or smaller to 500 μm may be considered as an additional cement with pozzolanic activity. It follows that the cement/aggregate ratio is close to 1/2 for these compositions and leading to the development of a higher strength.

The trends of water absorption of the mortar samples as a function of the aging time are reported in Figure 3b for the different compositions considered in this work. The reference composition displays

a value of 7.7% after 7 days of aging, 6.6% after 28 days, 5.1% after 90 days, 4.8% after 180 days and after 270 days, 4.7% after 360 days and 1100 days. Composition S250 exhibits a value of 5.3% after 7 days—The water absorption of this sample progressively decreases to 3.6% after 1100 days of aging. The sample S500 displays a similar trend with a water absorption of 6.9% after 7 days and 4.2% after 1100 days.

The water absorption of composition S1000 decreases from 7.7% after 7 days to 5.4% after 180 days. This decrease is followed by an increase of water absorption for longer immersion times, reaching 6.4% after 1100 days of aging. Similarly, composition S2500 displays an initial decrease from 7.9% after 7 days of aging to 5.5% after 90 days followed by a progressive increase of water absorption for longer aging times (7.5% after 1100 days).

It must be pointed out that water absorption tests are not a direct measurement of residual porosity since these tests enable only the evaluation of the open porosity of the material, while the total porosity remains undetermined. Moreover, further hydration might take place during the water absorption test, resulting in additional water absorption of the material. Nevertheless, it is observed that Figure 3b is consistent with Figure 3a, since water absorption data reflect the trend of materials strength for all compositions of the mortars.

Another important piece of evidence from the data reported in Figure 3 is that compositions S1000 and S2500 display an inversion of the trend of compression strength and water absorption after 180 days of aging. This inversion is reasonably related to the retarded hydration of some compounds and depends on the materials' permeability, which is a function of their open porosity. The retarded hydration occurs on hardened samples and, due to their small dimensions (100 mm), their expansion was not revealed by the investigation method followed in the present research. However, it can be expected that the addition of superfine slag to Portland cement improves the pore size distribution of the pastes and consequently the strength of the mortars because pore size and shape are crucial factors affecting their durability, as they influence penetration of liquids, vapors or gases into the matrix [32,33]. The time required for permeation falls between 180 and 360 days and depends on the preparation protocol followed rather than on materials composition.

Table 5 reports compressive strength data (averaged over 3 measurements) and their standard deviation for samples that underwent accelerated aging; that is, autoclave and thermal cycling processing. It can be observed that mortars R, S250 and S500 improve their strength after accelerated aging whereas, S1000 and S2500 compositions show a decrease of mechanical properties after accelerated aging. Data in Table 5 confirm that that strength values obtained after autoclave treatments are in good agreement with those obtained after thermal cycling. Moreover, these data further confirm that the use of slag with maximum size equal or smaller than 500 μm enables production of stable mortars, since their strength is higher than that measured after 28 days of aging. On the other hand, materials prepared using SS with larger size exhibit low strength. This indicates that a certain percentage of the volume expansion may close the porosity, making the entire bulk much more compact [34]. This effect is more evident for materials containing small particles that can be hydrated without destructive effects.

Table 5. Compressive strength (MPa) data of mortars samples after 28 days of aging (σ_{28}) and further subjected to autoclave test (σ_a) or 100 thermal cycles between −20 and +40 °C (σ_{tc}).

Mortar Composition	σ_{28}	σ_a	σ_{tc}
R	33 ± 2	36 ± 4	33 ± 3
S250	45 ± 4	47 ± 3	52 ± 4
S500	40 ± 3	43 ± 2	45 ± 3
S1000	36 ± 2	29 ± 6	26 ± 5
S2500	34 ± 4	20 ± 5	18 ± 4

Figure 4 is an optical stereomicroscope image of the free surface of a mortar sample with composition S2500 after the freezing and thawing cycles between −20° and +40 °C. Extended crazing

can be seen in the image. This is responsible for the strength reduction observed for this composition. A similar phenomenon, although less pronounced, was observed for composition S1000.

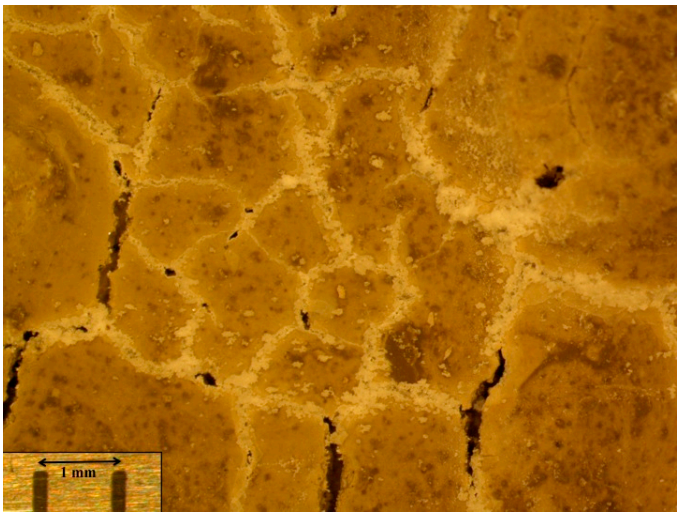

Figure 4. Optical stereomicroscope image of the free surface of a mortar sample S2500 after 100 cycles between −20°C and +40 °C.

After 28 days of aging, expansions of 0.032%, 0.019% and 0.025% were respectively measured for the reference composition, S250 and S500 samples, respectively. Mortars S1000 and S2500 showed an expansion of 0.043% and 0.047% respectively. All expansion values are below the 0.05% limit established by the ASTM C33 standard.

Based on chemical and crystallographic data discussed above, the starting slag has been classified as a material that could display hydraulic properties. However, their hydraulic efficiency should reasonably depend on the particle size distribution of the slag. In fact, it is generally accepted that the hydraulic activity of the powder becomes stronger when the particle size is decreased. This is supported by the compressive strength tests carried out in the present research. In particular, samples containing slag with maximum size equal or larger than 1000 μm display compressive strength lower than those of the blank composition. In contrast, samples containing slag with maximum size equal or smaller than 500 μm display higher strength values. This behaviour indicates that slags with maximum size equal or smaller than 500 μm can be almost completely considered as cementitious material. This leads to a modification of the cement/aggregate ratio improving the final strength of hydrated products. On the other hand, in compositions with maximum slag size equal or larger to 1000 μm, only a limited part of the slag could develop hydraulic activity during the early stages of materials hydration. Moreover, large slag particles impair the materials' stability after long term aging.

As a conclusive remark, it is possible to state that the use of SS in mortar production is possible provided that the maximum size of the slag is smaller than 500 μm. This results in an improved materials long term stability combined with high compressive strength.

4. Conclusions

The present research demonstrates that mortars prepared using a commercial CEMII/B-S 42.5N cement, a natural aggregate, steel slag with maximum size equal or smaller than 2500 μm, Glenium 51 as superplasticizer and water display good compression strength after aging for 7, 28, 90 and 180 days in water at 20 °C, when prepared following a modified protocol route with respect to those normally used for the production of mortars or concretes. However, if aged for longer times, samples containing slag with particles of size larger than 1000 μm exhibit a decrease of compressive strength after accelerated aging, due to localized expansion caused by the delayed hydration of some compounds contained in the starting slag. On the other hand, samples made with slag containing

particles with maximum size equal or smaller than 1000 μm display a compressive strength higher than the slag-free reference composition for all aging times.

Author Contributions: Stefano Maschio and Erika Furlani conceived and designed the experiments discussed in the paper. Moreover, they prepared the manuscript; Eleonora Aneggi carried out the X-ray experiments and analyzed the data; Alex Lanzutti and Maria Lekka contributed in the characterization of the mechanical behaviour of the materials; Lorenzo Fedrizzi and Francesco Andreatta contributed in the analysis of long term behaviour of the materials.

Conflicts of Interest: The authors declare no conflict of interest.

References

1. Barnes, P.; Fentiman, C.; Jeffery, J.W. Structurally related dicalcium silicate phases. *Acta Cristallogr. A Found. Crystallogr.* **1980**, *36*, 353–356. [CrossRef]
2. Birchal, V.S.; Rocha, S.D.; Ciminelli, V.S. The effect of magnesite calcination conditions on magnesia hydration. *Miner. Eng.* **2000**, *13*, 1629–1633. [CrossRef]
3. Chen, M.; Zhou, M.K.; Wu, S. Optimization of blended mortars using steel slag sand. *J. Wuhan Univ. Technol.* **2007**, *22*, 741–744. [CrossRef]
4. Lun, Y.; Zhou, M.K.; Cai, X.; Xu, F. Methods for improving volume stability of steel slag as fine aggregate. *J. Wuhan Univ. Technol.* **2008**, *23*, 737–742. [CrossRef]
5. Ben Haha, M.; Lothenbach, B.; Le Saout, G.; Winnefeld, F. Influence of slag chemistry on the hydration of alkali-activated blast-furnace slag—Part I: Effect of MgO. *Cem. Concr. Res.* **2011**, *41*, 955–963. [CrossRef]
6. Kuhn, M.; Drissen, P.; Geiseler, J.; Schrey, H.J. A new BOF slag treatment technology. In Proceedings of the 2nd European Oxygen Steel Making Congress, Taranto, Italy, 13–15 October 1997; pp. 445–453.
7. Shigeru, M.; Hirohi, K.; Keiichi, K. The development of the new aging process of steel-making slag. *SEAISI Q.* **1997**, *26*, 37–48.
8. Geiseler, J. Use of steel works slag in Europe. *Waste Manag.* **1996**, *16*, 59–63. [CrossRef]
9. Shi, C.; Hu, S. Cementitious properties of ladle slag fines under autoclave curing conditions. *Cem. Concr. Res.* **2003**, *33*, 1851–1856. [CrossRef]
10. Fleischanderl, A.; Gennari, U.; Ilie, A. ZEWA—Metallurgical process for treatment of residues from steel industry and other industrial sectors to generate valuable products. *Ironmak. Steelmak.* **2004**, *31*, 444–449. [CrossRef]
11. Monshi, A.; Asgarani, M.K. Producing Portland cement from iron and steel slag and limestone. *Cem. Concr. Res.* **1999**, *29*, 1373–1377. [CrossRef]
12. Akın Altun, İ.; Yılmaz, İ. Study on steel furnace slags with high MgO as additive in Portland cement. *Cem. Concr. Res.* **2002**, *32*, 1247–1249. [CrossRef]
13. Kourounis, S.; Tsivilis, S.; Tsakiridis, P.E.; Papadimitriou, G.D.; Tsibouki, Z. Properties and hydration of blended cements with steelmaking slag. *Cem. Concr. Res.* **2007**, *37*, 815–822. [CrossRef]
14. Shoaib, M.M.; Balaha, M.M.; Ahmed, S.A. Influence of aggregate type on mortar thermal stability. *Indian J. Eng. Mater. Sci.* **2000**, *7*, 217–224.
15. Manso, J.M.; Gonzalez, J.J.; Polanco, J.A. Electric Arc Furnace Slag in Concrete. *J. Mater. Civ. Eng.* **2004**, *16*, 639–645. [CrossRef]
16. Manso, J.M.; Losanez, M.; Polanco, J.A.; Gonzalez, J. Ladle furnace slag in construction. *J. Mater. Civ. Eng.* **2005**, *17*, 513–518. [CrossRef]
17. Manso, J.M.; Polanco, J.A.; Losanez, M.; Gonzalez, J.J. Durability of concrete made with EAF slag as aggregate. *Cem. Concr. Compos.* **2006**, *28*, 528–534. [CrossRef]
18. Qasrawi, H.; Shalabi, F.; Asi, I. Use of low CaO unprocessed steel slag in concrete as fine aggregate. *Constr. Build. Mater.* **2009**, *23*, 1118–1125. [CrossRef]
19. Shi, C.; Qian, J. High performance cementing materials from industrial slag-A review. *Resour. Conserv. Recycl.* **2000**, *29*, 195–207. [CrossRef]
20. Shi, C. Characteristics and cementitious properties of ladle slag fines from steel production. *Cem. Concr. Res.* **2002**, *32*, 459–462. [CrossRef]
21. Furlani, E.; Maschio, S. Long term compression strength of mortars produced using coarse steel slag as aggregate. *Adv. Civ. Eng.* **2016**, *2016*, 3431249. [CrossRef]

22. Faraone, N.; Tonello, G.; Furlani, E.; Maschio, S. Steelmaking slag as aggregate for mortars: Effects of particle dimension on compression strength. *Chemosphere* **2009**, *77*, 1152–1156. [CrossRef] [PubMed]
23. Wainwright, P.J.; Ait-Aider, H. The influence of cement source and slag additions on the bleeding of concrete. *Cem. Concr. Res.* **1995**, *25*, 1445–1456. [CrossRef]
24. Pèra, J.; Husson, S.; Guillot, B. Influence of finely ground limestone on cement hydration. *Cem. Concr. Res.* **1999**, *21*, 99–105. [CrossRef]
25. Jenkins, R.; Snyder, R. *Introduction to X-ray Powder Diffractometry*; Wiley: New York, NY, USA, 1996; ISBN 978-0471513391.
26. Mantel, D.G. Investigation into the hydraulic activity of five granulated blast furnace slags with eight different Portland cements. *ACI Mater. J.* **1994**, *91*, 471–477.
27. Smolczyk, H.G. The effect of chemistry of slag on the strength of blast furnace cements. *Zem-Kalk-Gips* **1978**, *31*, 294–296.
28. Hwang, C.L.; Lin, C.Y. Strength development of blended blast furnace slag cement mortars. In Proceedings of the 2nd International Conference on Fly Ash, Silica Fume, Slag and Natural Pozzolans in Concrete, Madrid, Spain, 21–26 April 1986; Malhotra, V.M., Ed.; American Concrete Institute: Detroit, MI, USA, 1986; Volume 2, pp. 1323–1340.
29. Pal, S.C.; Mukherjee, A.; Pathak, S.R. Investigation of hydraulic activity of ground granulated blast furnace slag in concrete. *Cem. Concr. Res.* **2003**, *33*, 1481–1486. [CrossRef]
30. Maslehuddin, M.; Sharif, A.M.; Shameem, M.; Ibrahim, M.; Barry, M.S. Comparison of properties of steel slag and crushed limestone aggregate concretes. *Constr. Build. Mater.* **2003**, *17*, 105–112. [CrossRef]
31. Gardner, L.J.; Bernal, S.A.; Walling, S.A.; Corkhill, C.L.; Provis, J.L.; Hyatt, N.C. Characterisation of magnesium potassium phosphate cements blended with fly ash and ground granulated blast furnace slag. *Cem. Concr. Res.* **2015**, *74*, 78–87. [CrossRef]
32. Kumar, S.; Kumar, R.; Bandopadhyay, A.; Alex, T.C.; Ravi Kumar, B.; Das, S.K.; Mehrotra, S.P. Mechanical activation of granulated blast furnace slag and its effect on the properties and structure of portland slag cement. *Cem. Concr. Compos.* **2008**, *30*, 679–685. [CrossRef]
33. Hajimohammadi, A.; van Deventer, J.S.J. Dissolution behaviour of source materials for synthesis of geopolymer binders: A kinetic approach. *Int. J. Miner. Process.* **2016**, *153*, 80–86. [CrossRef]
34. Wang, G.; Wang, Y.; Gao, Z. Use of steel slag as a granular material: Volume expansion prediction and usability criteria. *J. Hazard. Mater.* **2010**, *184*, 555–560. [CrossRef] [PubMed]